Research Project Report: Spin-Direction-Spin Coupling of Quasiguided Modes in Plasmonic Crystals

PH4214: RESEARCH PROJECT II

(Dated: May 10, 2025)

Nimish Sharma
21MS184

Instructor: Dr. Nirmalya Ghosh

CONTENTS

Abstract: This report summarizes a novel optical phenomenon, spin-direction-spin (SDS) coupling, demonstrated using quasi-guided modes in a wave-guided plasmonic crystal (WPC). The study reveals how spin-orbit interaction (SOI) effects such as the forward and inverse spin Hall effect of light (SHE) manifest in the far field via momentum-domain Mueller matrix analysis. By exploiting hybridized photonic-plasmonic Fano resonances and spatially varying polarization generated through nonparaxial focusing, the experiment uniquely demonstrates both input spin-controlled directionality and direction-induced spin acquisition in scattered light. The implications span fundamental optics to future spin-photonic devices.

I. INTRODUCTION

Spin-orbit interaction (SOI) of light, involving the interplay between spin angular momentum (SAM), orbital angular momentum (OAM), and linear momentum, has unlocked new phenomena and device paradigms in photonics. One such effect—spin-momentum locking—has been extensively studied, especially in evanescent fields and metasurfaces. The present work introduces an extension to this concept: *spin-direction-spin* coupling, simultaneously demonstrating forward and inverse spin Hall effects (SHE) of light in a unified and simple experimental system. The platform is a one-dimensional wave-guided plasmonic crystal (WPC) composed of a periodic gold grating atop an indium tin oxide (ITO) waveguide.

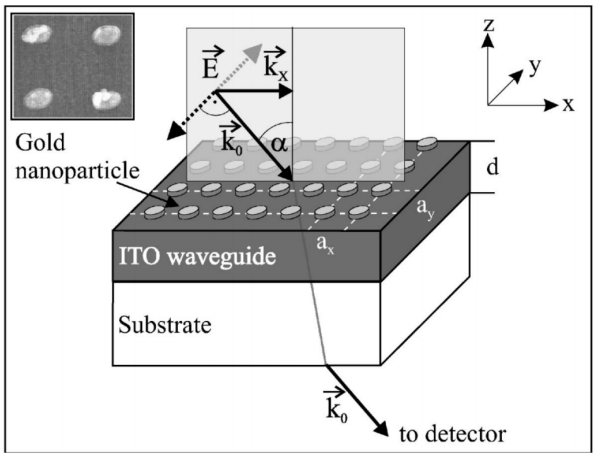

FIG. 1: *Visualization of the WPC crystal.*

II. THEORETICAL BACKGROUND

A. Spin-Orbit Interaction and Spin Hall Effects

SOI refers to the conversion or interaction of light's spin and orbital angular momentum. The forward SHE involves SAM-dependent trajectory deflection; conversely, the inverse SHE entails direction-dependent SAM acquisition. Traditionally, these are studied separately, but the SDS coupling phenomenon described here integrates them in a reciprocal and simultaneous fashion.

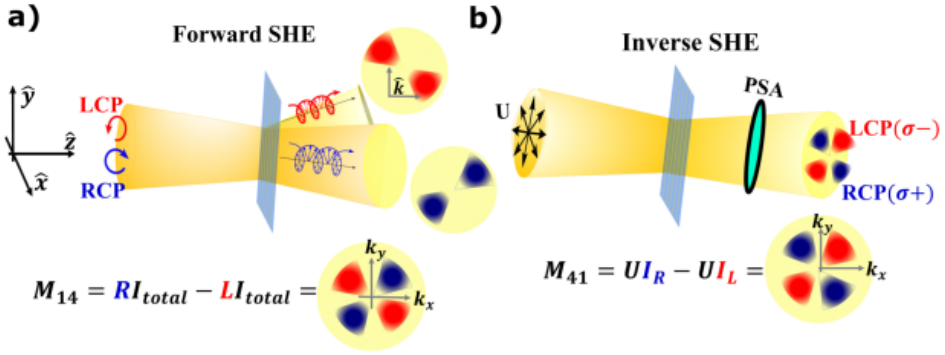

FIG. 2: *(a) Forward SHE depicting spin-dependent trajectory splitting of light. (b) Inverse SHE depicting direction-dependent spin acquisition of light.*

B. Spin-Momentum Locking

Spin-momentum locking in photonic systems refers to the intrinsic relation between the propagation direction and the transverse SAM of evanescent or guided waves. This leads to unidirectional excitation, depending on the spin state. However, in the current study, this effect is not merely locked in propagation direction; it is bidirectionally entangled with spin states both at input and output. We perform the Inverse Fourier Transform on certain elements of the Mueller Matrix to confirm the existence of leaky modes from the WPC through their radially decaying behaviour as shown in Figure 3.

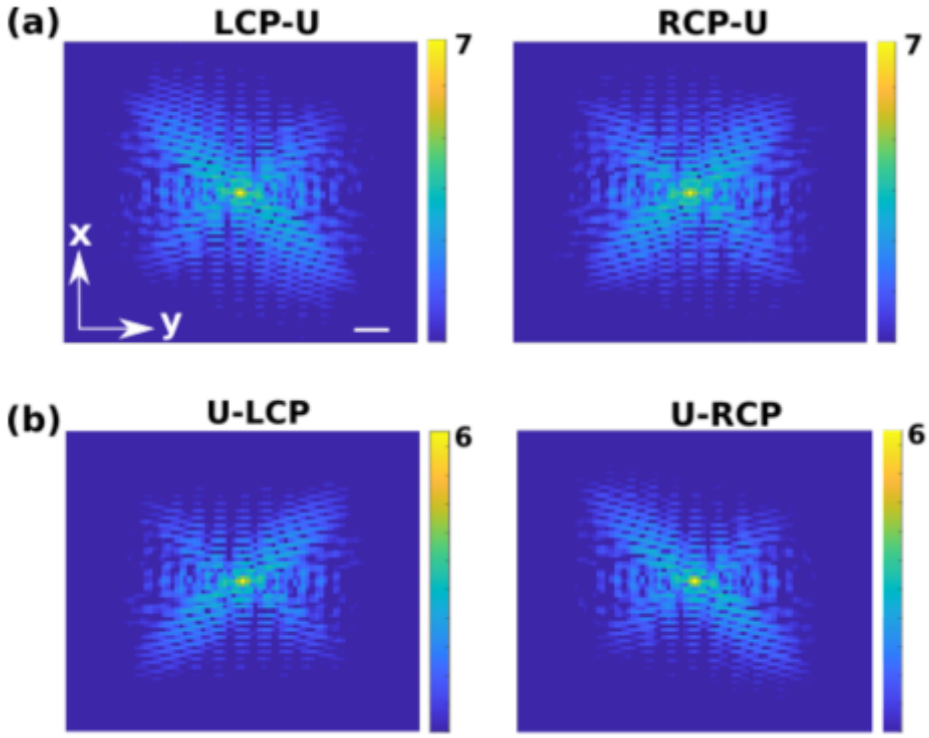

FIG. 3: *Inverse Fourier Transformed images of different elements of the Mueller Matrix. (a) IFT reveals spin-orbit coupling, which causes directional excitation of LCP and RCP, visible in opposite azimuthal lobes. (b) IFT reveals direction-dependent spin selection.*

C. Theoretical Modeling and Verification

Using Jones- and Mueller matrix formalisms, the experiment is modeled as a cascade of two linear diattenuating retarders: one from tight-focusing geometry with azimuthal anisotropy, and the other from the WPC with fixed anisotropy aligned to the grating. This modeling reproduces the experimental features of the Mueller matrix, including the azimuthal dependence on M_{14}, M_{41}, and other characteristic elements.

$$M_{\text{result}} = \begin{bmatrix} d_f d_{\text{wpc}} \cos(2\phi) + 1 & d_f \cos(2\phi) + d_{\text{wpc}}(x_f \sin^2(2\phi) \cos\delta_f + \cos^2(2\phi)) & (d_f - d_{\text{wpc}}(x_f \cos\delta_f - 1)\cos(2\phi))\sin(2\phi) & -d_{\text{wpc}} x_f \sin\delta_f \sin(2\phi) \\ d_f \cos(2\phi) + d_{\text{wpc}} & d_f d_{\text{wpc}} \cos(2\phi) + x_f \sin^2(2\phi)\cos\delta_f + \cos^2(2\phi) & (d_f d_{\text{wpc}} - x_f \cos\delta_f \cos(2\phi) + \cos(2\phi))\sin(2\phi) & -x_f \sin\delta_f \sin(2\phi) \\ d_f x_{\text{wpc}} \sin(2\phi)\cos\delta_{\text{wpc}} & x_{\text{wpc}}(x_f \sin\delta_f \sin\delta_{\text{wpc}} - (x_f\cos\delta_f - 1)\cos\delta_{\text{wpc}}\cos(2\phi))\sin(2\phi) & x_{\text{wpc}}(-x_f \sin\delta_f \sin\delta_{\text{wpc}}\cos(2\phi) + (x_f\cos\delta_f\cos^2(2\phi) + \sin^2(2\phi))\cos\delta_{\text{wpc}}) & x_f x_{\text{wpc}}(-2\sin\delta_f \sin^2\phi\cos\delta_{\text{wpc}} + \sin(\delta_f + \delta_{\text{wpc}})) \\ -d_f x_{\text{wpc}} \sin\delta_{\text{wpc}} \sin(2\phi) & x_{\text{wpc}}(x_f \sin\delta_f \cos\delta_{\text{wpc}} + (x_f\cos\delta_f - 1)\sin\delta_{\text{wpc}}\cos(2\phi))\sin(2\phi) & x_{\text{wpc}}(-x_f \sin\delta_f \cos\delta_{\text{wpc}}\cos(2\phi) - (x_f\cos\delta_f\cos^2(2\phi) + \sin^2(2\phi))\sin\delta_{\text{wpc}}) & x_f x_{\text{wpc}}(2\sin\delta_f \sin\delta_{\text{wpc}}\sin^2\phi + \cos(\delta_f + \delta_{\text{wpc}})) \end{bmatrix}$$

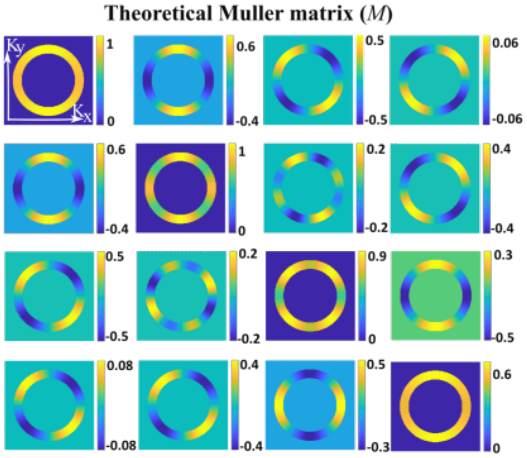

(A) *Theoritical Momentum domain Mueller Matrix*

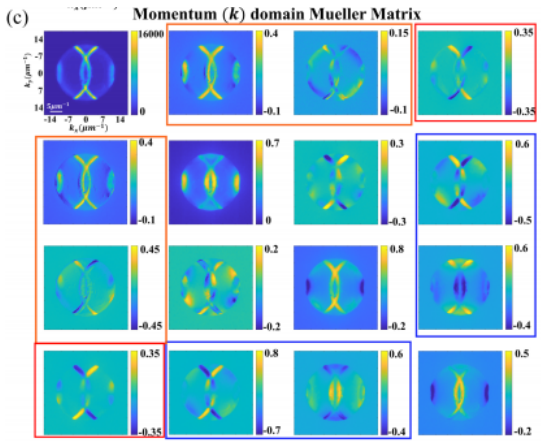

(B) *Experimentally obtained k domain Mueller Matrix*

FIG. 4: *Satisfactory results from the theoretical modelling obtained in the experimentally observed Mueller Matrix.*

III. EXPERIMENTAL SYSTEM AND METHODOLOGY

A. Waveguided Plasmonic Crystal Structure

The WPC consists of periodic Au gratings (550 nm period, 90 nm width, 20 nm thickness) deposited on a 190 nm ITO waveguiding layer over a glass substrate. The system supports hybridized leaky modes formed from coupling between the plasmonic and photonic resonances. This hybridisation induces asymmetric Fano resonances with polarisation-dependent amplitude and phase characteristics.

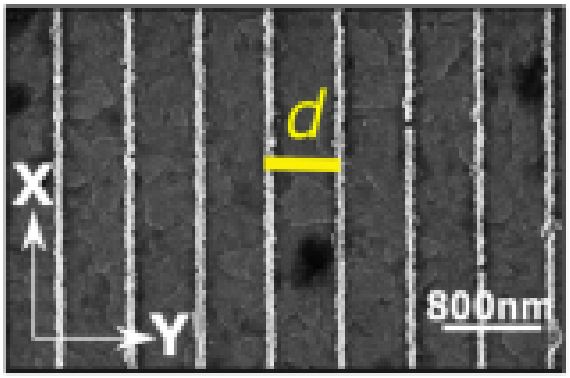

FIG. 5: *A typical Scanning Electron Microscope (SEM) Image of the WPC.*

B. Dark-Field Mueller Matrix Microscopy

A custom-built dark-field microscopy setup collects only scattered light and enables excitation of nonparaxial components via a high numerical aperture (NA) (0.8–0.92) condenser. The complete 4×4 Mueller matrix is derived through 36 polarization-resolved intensity measurements using combinations of linear and circular polarizations. Fourier-plane imaging permits spatially and spectrally resolved polarization analysis in k-space.

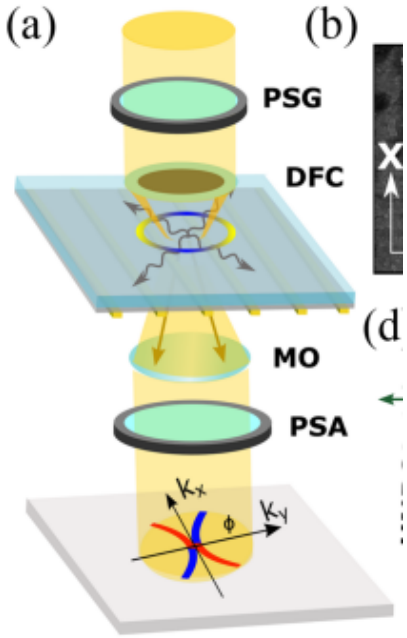

FIG. 6: *Dark field Mueller matrix imaging setup.*
PSG(Polarization state generator) : Rotatable Linear Polarizer + Achromatic Quarter Wave Plate (QWP)
DFC : Dark field Condenser
MO : Microscope objective lens
PSA(Polarization state analyzer) : Rotatable Linear Polarizer + Achromatic QWP

IV. OBSERVATION AND INTERPRETATION OF SDS COUPLING

A. Signature of Quasiguided Modes

The leaky modes generate arc-like k-space diffraction patterns because of broken symmetry and mode hybridization as shown in Figure 7. This arises due to $|k_w| > |k_0 \cdot NA|$ & $|k_w - G| < |k_0 \cdot NA|$, where G is the grating vector. These arcs encode SOI information and are modulated based on the incident and analyzed polarization states.

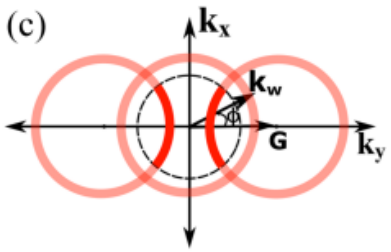

FIG. 7: *Idealised arc-like pattern of the WG modes.*

B. Forward and Inverse Spin Hall Effects

The forward SHE is manifested as input circular polarization-dependent azimuthal lobes in the scattered intensity, encoded in the Mueller matrix element M_{14}. The inverse SHE, probed via the M_{41} element, shows that even unpolarized input leads to spin-polarized scattered light—demonstrating a direction-spin coupling effect.

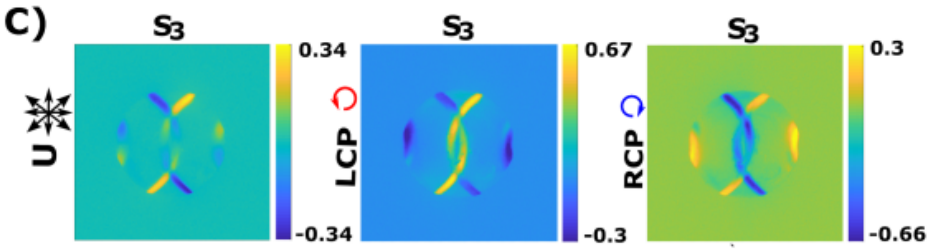

FIG. 8: *Unchanged lobe patterns for different input polarization states showing strong proof for Inverse SHE.*

These elements are described analytically as:

$$M_{14} = -d_{\mathrm{WPC}}\sqrt{1-d_f^2}\,\sin(\delta_f)\,\sin(2\phi) \tag{1}$$

$$M_{41} = d_f\sqrt{1-d_{\mathrm{WPC}}^2}\,\sin(\delta_{\mathrm{WPC}})\,\sin(2\phi) \tag{2}$$

V. ROLE OF FANO RESONANCES AND POLARIZATION ANISOTROPY

Fano resonances emerge from interference between narrow waveguide and broad plasmonic modes. These resonances enhance the anisotropy parameters d_{WPC} and δ_{WPC}, thereby strengthening the SDS effects. At resonance ($\lambda \approx 530\,\mathrm{nm}$), lobed intensity patterns in Mueller matrix elements are more pronounced compared to off-resonance wavelengths (e.g., 440 nm).

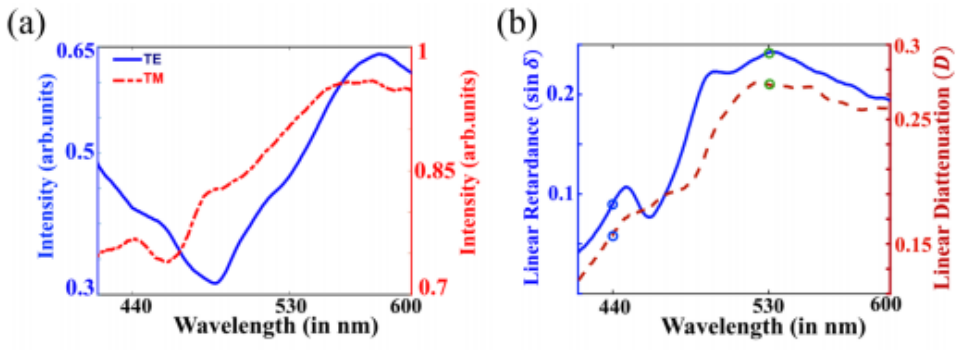

FIG. 9: *Enhancement of amplitude (diattenuation) and phase (retardance) anisotropy of WPC around the Fano spectrum.*

The spectrally asymmetric Fano line shapes further indicate differential mode hybridization for TE and TM polarizations, contributing to the distinct spin-selective responses. Performing the Finite element method (FEM), we observe highly confined near-fields for TE modes in ITO layer implying excitation of TE modes as show in Figure 10. We can also see reduced field confinement away from the Fano spectrum and hence, reduced hybridization.

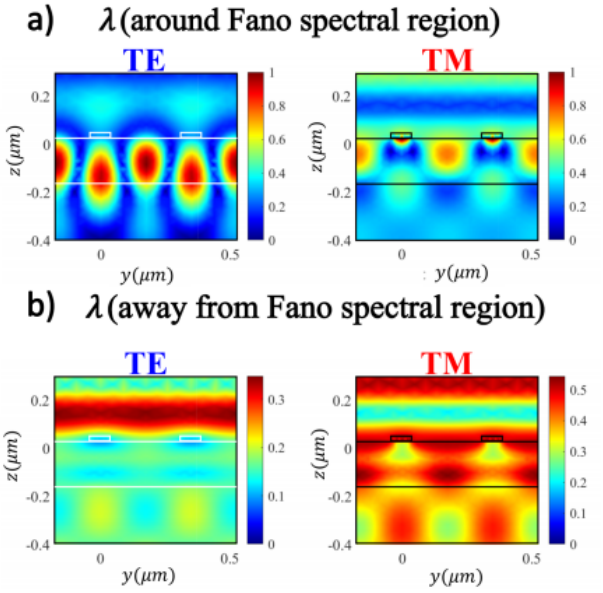

FIG. 10: *FEM simulation of near field distribution of hybridized WPC*

VI. IMPLICATIONS AND OUTLOOK

The demonstration of SDS coupling in a simple WPC platform opens avenues for:

- Compact spin-controlled directional couplers

- Spin-based optical information processing
- Polarization sorting and filtering at sub-wavelength scales

Moreover, the ability to utilize unpolarized light to achieve directionally spin-polarized emission presents a paradigm shift for passive photonic components, which could be employed in low-power, on-chip optical routing and signal encoding. Such capabilities hold promise for integration into quantum photonic circuits where spin states of light can serve as carriers of quantum information.

The momentum-domain Mueller matrix technique introduced in this work further offers a robust and generalizable experimental framework for characterizing SOI phenomena in various nanostructures—including metasurfaces, photonic crystals, and topological photonic systems. This approach could also be extended to dynamically reconfigurable or nonlinear materials, enabling real-time manipulation and control of light's angular momentum properties.